Full-Wave Boundary Integral Equation Method for Suspended Planar Transmission Lines with Pedestals and Finite Metallization Thickness

Lei Zhu, *Student Member, IEEE,* and Eikichi Yamashita, *Fellow, IEEE*

***Abstract*—A new boundary integral equation method is proposed for the full-wave analysis of suspended planar transmission lines with pedestals and/or finite metallization thickness. Coupled boundary integral equations are formulated on the equivalent magnetic currents only on the apertures of subregions using the Green's identity of the second kind. Because it is possible to take a large number of terms in the series expansion of Green's functions in each subregion independently from the order of resulting matrices, this approach can avoid the relative convergence problem. Numerical results of the present method on suspended coplanar waveguides are found to have a stable convergent property and to be in excellent agreement with other available theoretical results. Numerical data reveal the effects of conductor thickness and aperture width on the transmission properties of suspended planar transmission lines with pedestals.**

I. Introduction

SUSPENDED planar transmission lines with pedestals and/or grooves have recently been studied as new promising transmission structures [1]–[3]. Compared with conventional planar transmission lines, they possess low propagation losses and weak dispersion due to the distribution of electromagnetic energy into the air region. In addition, they still retain the merits of easy fabrication and planar configuration. The transmission properties of such suspended striplines with grooves and/or pedestals have been treated with the quasi-TEM wave approximation [1] and with the full-wave analysis without considering finite strip conductor thickness [2]–[3].

In the analysis of electromagnetic boundary-value problems, the boundary integral equation method has been extensively employed in the past to derive the cutoff wavelengths of various waveguides, scattering parameters of waveguide discontinuities, and radiation properties of various antennas. With the assumption of the quasi-TEM wave propagation, the boundary integral equation method with different basis functions has been applied to analyze the characteristics of microstrip lines [4] and coplanar waveguides [5]. The versatility of the Green's function makes it possible to use the boundary integral approach to find solutions for various structures with complex cross-sections [6]–[8], for instance, a trapezoidal transmission line or a microstrip line of arbitrary cross section. In addition, the eigen-function weighted boundary integral equation method has been proposed for the rigorous analysis of dispersion characteristics of various planar transmission lines with finite metallization thickness such as microstrip lines, conductor-backed coplanar waveguides and micro-coplanar strip lines [9]–[10].

In this paper, a full-wave boundary integral equation method is presented for the rigorous analysis of planar transmission lines with pedestals and/or finite metallization thickness. A coupled set of boundary integral equations is set up based on the Green's identity of the second kind as a process of the boundary integration approach. Two kinds of simple scalar Green's functions corresponding to the TM-mode and the TE-mode are selected for each shielded subregion. It is expected that the overall boundary integration contours are reduced to only those at the apertures between two adjacent subregions to result in shorter computation time. Unknown functions in the integral equations are also limited to those of equivalent magnetic currents only at the aperture surface.

II. Formulation of Boundary Integral Equations

Fig. 1(a) depicts the cross-sectional geometry of a generalized suspended planar transmission line with pedestals and/or finite metallization thickness. Many well-known planar transmission lines can be constructed easily from this prototype structure by properly changing sizes. Although their propagation characteristics have been studied extensively using the transverse resonance method and an experimental method without considering strip thickness [3], there still remain unsolved problems, such as the effects of the conductor thickness and aperture width on the transmission properties.

Only half of the general structure in Fig. 1(a) with an equivalent magnetic wall has to be considered because of the symmetry of the cross-section, which is shown in Fig. 1(b). The free-space Green's function is usually chosen for building boundary integral equations in the traditional boundary integral approach. As for the structure with a complex boundary configuration like Fig. 1(b), a large system of boundary integral equations will be necessitated according to the above traditional approach. This may be a principal reason why the boundary integral approach is hardly extended to the full-wave analysis of various planar transmission lines until now.

The whole cross-section is firstly divided into four rectangular homogeneous subregions for the cross-sectional geometry with multiple rectangular subregions. A pair of scalar Green's functions for each subregion corresponding to the TM-mode and the TE-mode are constructed based on the basic solutions of the Helmholtz's equation and the homogeneous boundary conditions for a shielded rectangular subregion. These Green's

Manuscript received April 3, 1992; revised July 6, 1992.

The authors are with the Department of Electronic Engineering, University of Electro-Communications, Chofugaoka 1-5-1, Chofu-Shi, Tokyo 182, Japan.

IEEE Log Number 9205499.

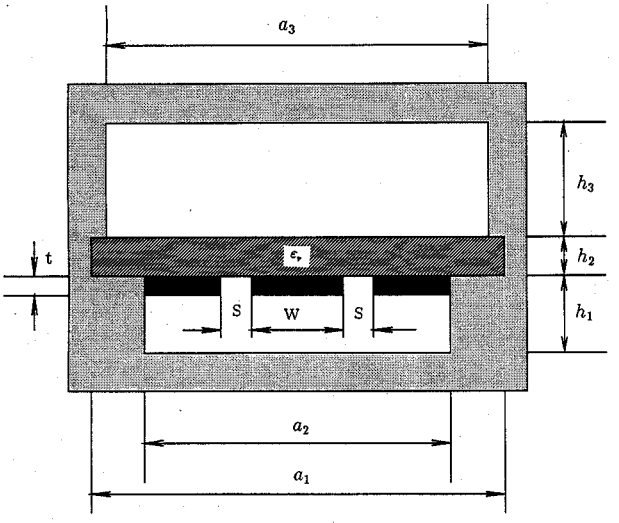

(a)

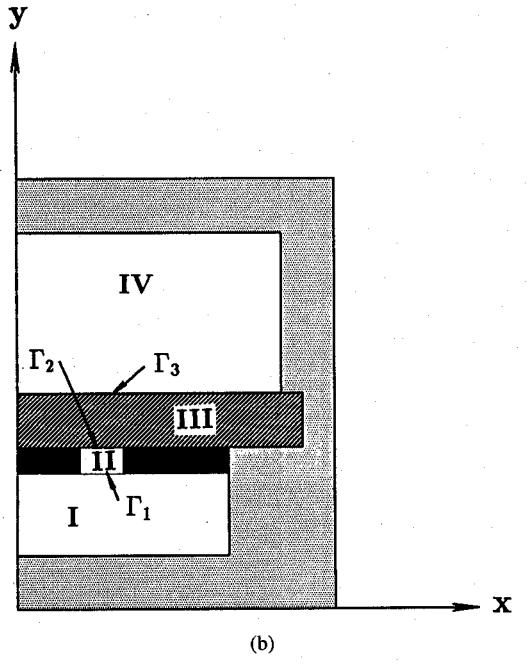

(b)

Fig. 1. Shielded suspended planar transmission lines with pedestals. (a) Cross-sectional geometry. (b) A half of the cross-section to be analyzed.

functions are expressed as follows:

$$G_i^e(x, x_s, y, y_s) = \sum p_i^m(x, x_s, y, y_s) \tag{1a}$$

$$G_i^h(x, x_s, y, y_s) = \sum g_i^m(x, x_s, y, y_s) \tag{1b}$$

where the symbols, $p_i^m(x, x_s, y, y_s)$ and $q_i^m(x, x_s, y, y_s)$, denote the mth term in the above two Green's functions in the ith subregion and are given by (2a) and (2b) at the bottom of the page and

$$S_m(y, y_s) = \begin{cases} \dfrac{\cos\left[k_{ym}^i(y - h_i)\right]\cos\left[k_{ym}^i y_s\right]}{\sin\left[k_{ym}^i h_i\right]} & (y > y_s) \\ \dfrac{\cos\left[k_{ym}^i y\right]\cos\left[k_{ym}^i(y_s - h_i)\right]}{\sin\left[k_{ym}^i h_i\right]} & (y < y_s) \end{cases} \tag{3a}$$

$$T_m(y, y_s) = \begin{cases} \dfrac{\sin\left[k_{ym}^i(y - h_i)\right]\sin\left[k_{ym}^i y_s\right]}{\sin\left[k_{ym}^i h_i\right]} & (y > y_s) \\ \dfrac{\sin\left[k_{ym}^i y\right]\sin\left[k_{ym}^i(y_s - h_i)\right]}{\sin\left[k_{ym}^i h_i\right]} & (y < y_s) \end{cases} \tag{3b}$$

where a_i, h_i and k_{ym}^i denote the width, the height, and the propagation constant in the y direction for the ith rectangular subregion, while (x, y) and (x_s, y_s) are the coordinates of a field point and a source point, respectively.

Based on the Green's identity of the second kind,

$$\int\int_S [G(r, r_s)\nabla_\perp^2 \Phi(r_s) - \nabla_\perp^2 G(r, r_s)\Phi(r_s)]dS = \int_\Gamma \left[G(r, r_s)\frac{\partial \Phi(r_s)}{\partial n_s} - \frac{\partial G(r, r_s)}{\partial n_s}\Phi(r_s)\right] d\Gamma \tag{4}$$

a pair of boundary integral equations corresponding to the TM-mode and the TE-mode can be set up with integrals on dielectric interfaces or apertures between two adjacent subregions as follows:

$$E_z(r) = -\int_\Gamma \frac{\partial G^e(r, r_s)}{\partial n_s} E_z(r_s) d\Gamma \tag{5a}$$

$$H_z(r) = \int_\Gamma G^h(r, r_s)\frac{\partial H_z(r_s)}{\partial n_s} d\Gamma \tag{5b}$$

where, G^e and G^h denote the two kinds of Green's functions, respectively, corresponding to the TM-mode and the TE-mode. r and r_s denote the field and source position, respectively.

$$p_i^m(x, x_s, y, y_s) = -\frac{2S_m(y, y_s)}{a_i k_{ym}^i} \times \begin{cases} \cos\left[\dfrac{(2m-1)\pi x}{a_i}\right]\cos\left[\dfrac{(2m-1)\pi x_s}{a_i}\right] & (m = 1, 2, \cdots, \infty) \\ & i \in I, III, IV \\ \sin\left[\dfrac{m\pi(x - w/2)}{s}\right]\sin\left[\dfrac{m\pi(x_s - w/2)}{s}\right] & (m = 1, 2, \cdots, \infty) \\ & i \in II \end{cases} \tag{2a}$$

$$q_i^m(x, x_s, y, y_s) = -\frac{2T_m(y, y_s)}{a_i k_{ym}^i} \times \begin{cases} \sin\left[\dfrac{(2m-1)\pi x}{a_i}\right]\sin\left[\dfrac{(2m-1)\pi x_s}{a_i}\right] & (m = 1, 2, \cdots, \infty) \\ & i \in I, III, IV \\ \cos\left[\dfrac{m\pi(x - w/2)}{s}\right]\cos\left[\dfrac{m\pi(x_s - w/2)}{s}\right] & (m = 0, 1, \cdots, \infty) \\ & i \in II \end{cases} \tag{2b}$$

Since the Green's functions and field component functions satisfy the same tangential field continuity conditions on shielded rectangular surfaces except aperture surfaces, only apertures remain as necessary boundary integral areas. On the other hand, according to the equivalence principle [11], electric fields on the jth aperture can be replaced by equivalent magnetic surface currents in opposite directions, M^j and $-M^j$, flowing on the two sidewalls of a perfectly conducting plane. The magnetic field components in the four subregions are expressed as follows with simple integral formulas of the equivalent magnetic currents using the relation derived from Maxwell's equations:

$$H_x^I(x,y) = -\left[\int_{\Gamma_1} G_I^{11} M_z^1 dx_s + \int_{\Gamma_1} G_I^{12} M_x^1 dx_s\right] \quad (6a)$$

$$H_z^I(x,y) = -\left[\int_{\Gamma_1} G_I^{21} M_z^1 dx_s + \int_{\Gamma_1} G_I^{22} M_x^1 dx_s\right] \quad (6b)$$

$$H_x^{II}(x,y) = \left[\int_{\Gamma_1} G_{II}^{11} M_z^1 dx_s + \int_{\Gamma_1} G_{II}^{12} M_x^1 dx_s\right] - \left[\int_{\Gamma_2} G_{II}^{11} M_z^2 dx_s + \int_{\Gamma_2} G_{II}^{12} M_x^2 dx_s\right] \quad (6c)$$

$$H_z^{II}(x,y) = \left[\int_{\Gamma_1} G_{II}^{21} M_z^1 dx_s + \int_{\Gamma_1} G_{II}^{22} M_x^1 dx_s\right] - \left[\int_{\Gamma_2} G_{II}^{21} M_z^2 dx_s + \int_{\Gamma_2} G_{II}^{22} M_x^2 dx_s\right] \quad (6d)$$

$$H_x^{III}(x,y) = \left[\int_{\Gamma_2} G_{III}^{11} M_z^2 dx_s + \int_{\Gamma_2} G_{III}^{12} M_x^2 dx_s\right] - \left[\int_{\Gamma_3} G_{III}^{11} M_z^3 dx_s + \int_{\Gamma_3} G_{III}^{12} M_x^3 dx_s\right] \quad (6e)$$

$$H_z^{III}(x,y) = \left[\int_{\Gamma_2} G_{III}^{21} M_z^2 dx_s + \int_{\Gamma_2} G_{III}^{22} M_x^2 dx_s\right] - \left[\int_{\Gamma_3} G_{III}^{21} M_z^3 dx_s + \int_{\Gamma_3} G_{III}^{22} M_x^3 dx_s\right] \quad (6f)$$

$$H_x^{IV}(x,y) = \left[\int_{\Gamma_3} G_{IV}^{11} M_z^3 dx_s + \int_{\Gamma_3} G_{IV}^{12} M_x^3 dx_s\right] \quad (6g)$$

$$H_z^{IV}(x,y) = \left[\int_{\Gamma_3} G_{IV}^{21} M_z^3 dx_s + \int_{\Gamma_3} G_{IV}^{22} M_x^3 dx_s\right] \quad (6h)$$

where M_x^j and M_z^j are the two components of the equivalent magnetic surface currents on the jth aperture $\Gamma_j (j = 1, 2, 3)$. H_x^i and H_z^i denote the two components of magnetic fields in the ith subregion (i = I, II, III, IV), while the symbols, $G_i^{11}, G_i^{12}, G_i^{21}$ and G_i^{22}, denote four terms of the dyadic Green's function, which are defined by using the m-th term q_i^m of the magnetic Green's functions as:

$$G_i^{11} = \beta \sum_m \frac{\partial q_i^m}{\partial x} \quad (7a)$$

$$G_i^{12} = \sum_m \frac{\epsilon_r^i k_0^2 - k_{xm}^2}{k_{xm}^2} \frac{\partial^2 q_i^m}{\partial x \partial x_s} \quad (7b)$$

$$G_i^{21} = k_{ci}^2 \sum_m q_i^m \quad (7c)$$

$$G_i^{22} = \beta \sum_m \frac{\partial q_i^m}{\partial x_s} \quad (7d)$$

Based on the continuity of tangential magnetic components on each aperture surface between two adjacent subregions, a pair of general boundary integral formulas on the ith aperture can be formulated using the Galerkin's method as

$$\int_{\Gamma_i} \omega_x^i [H_x(x, y_i^+) - H_x(x, y_i^-)] dx = 0 \quad (8a)$$

$$\int_{\Gamma_i} \omega_z^i [H_z(x, y_i^+) - H_z(x, y_i^-)] dx = 0. \quad (8b)$$

A system of coupled homogeneous boundary integral equations are constructed by substituting (6) into (8), in which only equivalent magnetic currents remain as the unknown functions. In the mixed spectral domain approach [2], the transverse magnetic fields across the aperture have to be transformed into the space domain by the inverse Fourier transform because of the existence of different transform variables on the two sides of the apertures. The present method carries out all of the analysis processes only in the space domain, therefore, can omit the complex Fourier transform, and can treat piecewise rectangular cross-section problems easily.

In practical computations, the number of terms in the series expressions of the Green's functions and the magnetic currents are taken as finite, namely, N_1, N_2, N_3 and N_4, for the four subregions and, M_1, M_2 and M_3, on the three apertures, respectively. Choice of the number N is completely independent from the number M. Therefore, this approach does not lead to numerical instabilities or relative convergence problems like the mode-matching method as discussed in [12]. Simple sine and cosine functions are selected as the basis functions for equivalent magnetic currents. These functions can also expres the accurate solutions of magnetic currents in the analysis of the suspended planar transmission lines with grooves and/or pedestals. Moreover, the same functions are chosen as the weighting functions with the same number of basis function on the three apertures, that is, M_1, M_2 and M_3. Consequently, the coupled boundary integral equations are simplified as the following form through numerical discretizations:

$$\begin{bmatrix} [A_{11}] & [B_{11}] & [A_{12}] & [B_{12}] & [0] & [0] \\ [C_{11}] & [D_{11}] & [C_{12}] & [D_{12}] & [0] & [0] \\ [A_{21}] & [B_{21}] & [A_{22}] & [B_{22}] & [A_{23}] & [B_{23}] \\ [C_{21}] & [D_{21}] & [C_{22}] & [D_{22}] & [C_{23}] & [D_{23}] \\ [0] & [0] & [A_{32}] & [B_{32}] & [A_{33}] & [B_{33}] \\ [0] & [0] & [C_{32}] & [D_{32}] & [C_{33}] & [D_{33}] \end{bmatrix} \begin{bmatrix} [X_1] \\ [Z_1] \\ [X_2] \\ [Z_2] \\ [X_3] \\ [Z_3] \end{bmatrix} = [0] \quad (9)$$

where the symbols, $[X_j]$ and $[Z_j]$, denote the unknown submatrices about the two equivalent magnetic currents in the jth aperture. $[A_{ij}], [B_{ij}], [C_{ij}]$ and $[D_{ij}]$ are four coefficient submatrices with the unknown propagation constant indicating the effect of the magnetic currents in the jth aperture on the fields in the ith aperture. Each element of coefficient sub-matrices is written as

$$A_{ij} = \begin{cases} S_{ij}^{11} + S_{jj}^{11} & (i = j) \\ -S_{ij}^{11} & (i \neq j) \end{cases} \quad (10a)$$

$$B_{ij} = \begin{cases} S_{ii}^{12} + S_{jj}^{12} & (i = j) \\ -S_{ij}^{12} & (i \neq j) \end{cases} \quad (10b)$$

$$C_{ij} = \begin{cases} S_{ii}^{21} + S_{jj}^{21} & (i = j) \\ -S_{ij}^{21} & (i \neq j) \end{cases} \quad (10c)$$

$$D_{ij} = \begin{cases} S_{ii}^{22} + S_{jj}^{22} & (i = j) \\ -S_{ij}^{22} & (i \neq j) \end{cases} \tag{10d}$$

where the subscripts, ii and jj, denote two subregions above and below the ith or jth aperture in the case $(i = j)$, and ij denotes the subregion between the ith and jth aperture. The quantities, $S_{ij}^{11}, S_{ij}^{12}, S_{ij}^{21}$ and S_{ij}^{22}, are defined in the Appendix.

The summation form of Green's functions will disappear naturally with the orthogonal property of basis and weighting functions with the same sine or cosine functions in subregions II and IV. These facts also decrease computation time. In addition, such basis functions as the sine and cosine forms can also be applied directly to derive the propagation properties of the fundamental mode and higher-order modes in this method.

Like the mixed spectral domain method, this approach reduces the integration area of unknown functions only to apertures between two adjacent subregions. This results in the decrease of the number of unknown functions, a small system of equations, and can avoid relative convergence problems in the transverse resonance method or the mode matching method, seen in the case of a small aperture width of planar transmission lines as coplanar waveguides and fin-lines.

III. Numerical Results

The above-mentioned approach can be applied to analyze the transmission properties of various suspended planar transmission lines with grooves, pedestals, and/or finite metallization thickness. Fig. 2 shows the comparison of numerical results obtained by the present method with those given in [3] for the fundamental and the second order mode of the nonsymmetrically suspended substrate stripline in the case of zero-thickness conductor. Fig. 3 shows the dispersion characteristics of the shielded suspended coplanar waveguide with strip thickness $t = 0$ and $t = 130\,\mu$m, the difference between our results and the data given in [13] is less than 1.0%.

For the structure as shown in Fig. 1, the number of terms in the truncated series of Green's functions are proportional to the widths of each rectangular subregion, while the number of the magnetic current terms on the three apertures are chosen as the same value M. In the case of $M = 4$, the number N in the subregion I should be larger than 20 for the aperture width $s = 0.6$ mm and 120 for $s = 0.1$ mm to lead to accurate converging solutions for the suspended coplanar waveguides with $a_1 = 4.8$ mm, $a_2 = 6.5$ mm, $a_3 = 5.5$ mm, $\epsilon_r = 10.5, h_1 = h_3 = 2.54$ mm, $h_2 = 1.27$ mm, $w = 1.2$ mm. On the other hand, if $N = 400, M$ larger than 3 ensures high calculation accuracy. The above-mentioned points are shown clearly in Fig. 4 indicating the effective dielectric constants versus N and M. It is found in Fig. 4 that taking $N = 400$ and $M = 4$ is enough to derive satisfactory numerical solutions with computation time of 1 minute on a Sun 4 workstation for one frequency point. To obtain stable solutions for different subregions of a large ratio widths such as the case of $s = 0.1$ mm, the present method can be very effective compared with other methods in the sense of a small number of unknown functions and low order matrices.

Figs. 5 and 6 provide three dispersion curves for suspended planar transmission lines with strip thickness $t = 1, 40$, and

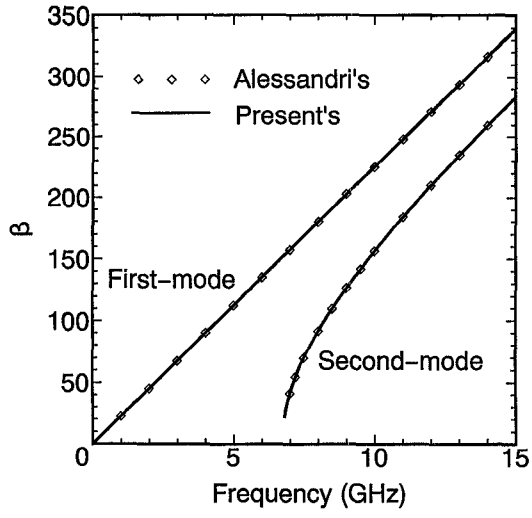

Fig. 2. Comparison of the propagation constants of the nonsymmetrically suspended substrate stripline calculated by the present method with those given in [3] for the fundamental and the second order mode. $a_1 = 15.8$ mm, $a_2 = 23.86$ mm, $a_3 = 22.86$ mm, $\epsilon_r = 2.2, h_1 = 2.286$ mm, $h_2 = 0.254$ mm, $h_3 = 11.43$ mm, $w = 10$ mm, $s = 2.9$ mm.

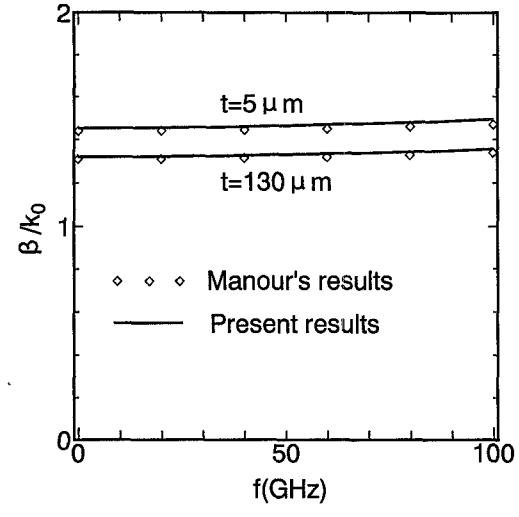

Fig. 3. Comparison of the propagation constants of the suspended coplanar waveguide calculated by the present method with those given in [13] $a_1 = a_2 = a_3 = 1.55$ mm, $\epsilon_r = 3.75, h_1 = h_3 = 1.44$ mm, $h_2 = 0.22$ mm, $w = s = 0.2$ mm.

100 μm, respectively, for $s = 0.6$ mm and $s = 0.1$ mm. It is found in Figs. 5 and 6 that the effect of strip conductor thickness becomes significant with the decrease of aperture width, especially in the case of small aperture widths. The above results indicate that even a small strip thickness gives appreciable effects on the transmission properties in the case of small aperture widths.

Figs. 7 and 8 show the variation of the effective dielectric constant with regard to aperture widths for different values of the strip conductor thickness and with regard to the strip conductor thickness for different values of aperture widths, respectively, at $f = 1.0$ GHz. It is found in Fig. 8 that the increase of strip conductor thickness makes the field energy concentrate into the aperture of air subregion resulting in the reduction of the effective dielectric constants. Fig. 7 shows

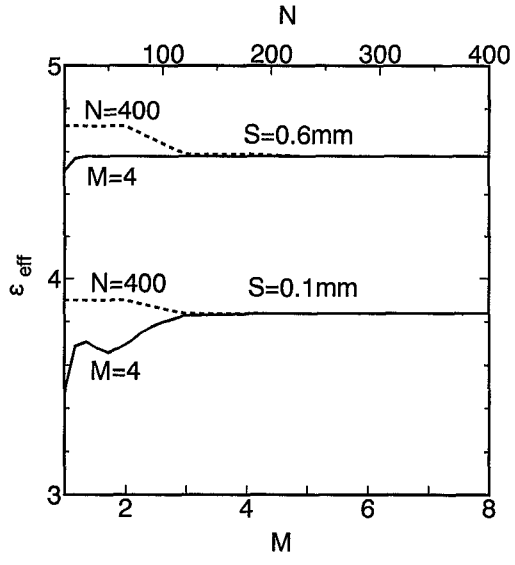

Fig. 4. Convergence properties with regard to the number of Green's function series terms and basis functions.

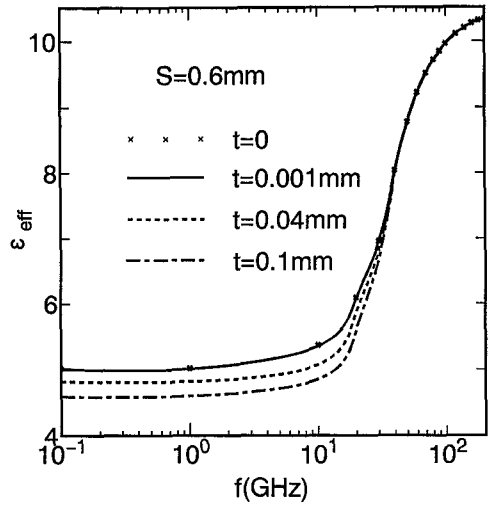

Fig. 5. Effective dielectric constants versus frequencies for $s = 0.6$ mm.

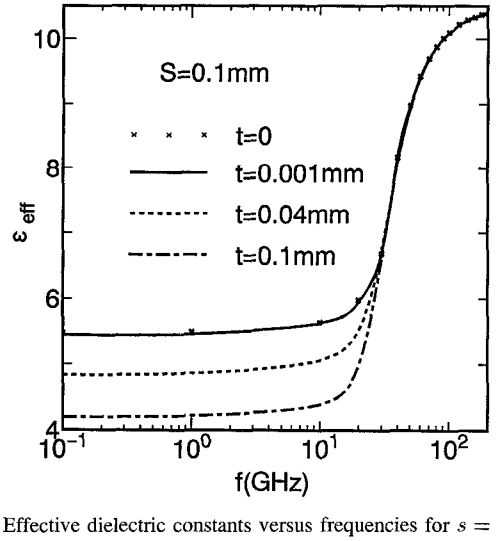

Fig. 6. Effective dielectric constants versus frequencies for $s = 0.1$ mm.

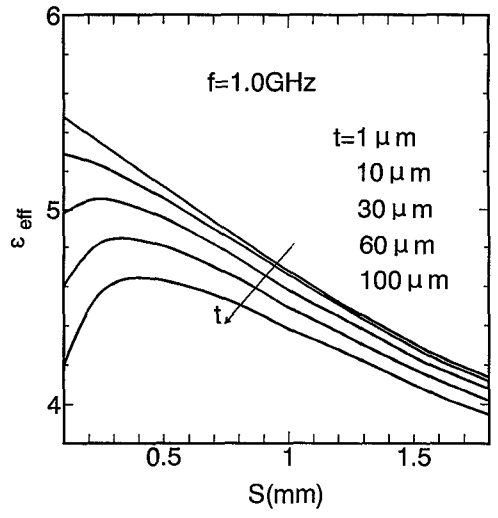

Fig. 7. Effective dielectric constants versus aperture widths for different values of strip conductor thickness.

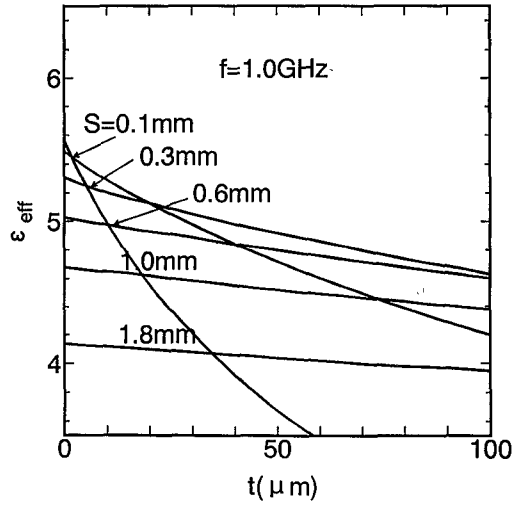

Fig. 8. Effective dielectric constants versus strip thickness for different aperture widths.

that the increase of the aperture width leads to the monotonous reduction of the effective dielectric constant in the case of zero-thickness strip conductor. However, the same increase results in a complex convex curve of the effective dielectric constant in the case of strip conductors of finite thickness due to the mixed effects of the aperture width and the strip conductor thickness.

IV. Conclusion

In this paper, we described a full-wave boundary integral equation method for the rigorous analysis of suspended planar transmission lines with pedestals and/or finite metallization thickness. Because it is possible for this method to take a large number of terms in the series expansion of Green's functions for each subregion independently from the order of resulting matrices, the approach can decrease the number of unknown functions, shorten computation time, and can avoid relative convergence problems. This method enables us to formulate a system of equations using simple Green's functions for each

subregion and to derive accurate solutions with a few terms of equivalent magnetic currents. The complex effects of both strip thickness and aperture width on transmission properties were discussed in detail. The versatility of the boundary integral approach makes this method useful to analyze the complex planar transmission lines with fairly arbitrary conductor configurations and substrate configurations.

APPENDIX

The sub-matrices, $S_{ij}^{11}, S_{ij}^{12}, S_{ij}^{21}$ and S_{ij}^{22}, in (10a) to (10d) are given by

$$S_{ij}^{11} = \int_{\Gamma_i}\int_{\Gamma_j} w_x^i(x) G_{ij}^{11}(x,x_s) u_x^j(x_s) dx_s dx \quad \text{(A1)}$$

$$S_{ij}^{12} = \int_{\Gamma_i}\int_{\Gamma_j} w_x^i(x) G_{ij}^{12}(x,x_s) u_z^j(x_s) dx_s dx \quad \text{(A2)}$$

$$S_{ij}^{21} = \int_{\Gamma_i}\int_{\Gamma_j} w_z^i(x) G_{ij}^{21}(x,x_s) u_x^j(x_s) dx_s dx \quad \text{(A3)}$$

$$S_{ij}^{22} = \int_{\Gamma_i}\int_{\Gamma_j} w_z^i(x) G_{ij}^{22}(x,x_s) u_z^j(x_s) dx_s dx \quad \text{(A4)}$$

where the four terms, $G_{ij}^{11}, G_{ij}^{12}, G_{ij}^{21}$ and G_{ij}^{22}, can be derived directly from (7), while the weighting functions, $w_x^i(x)$ or $w_z^i(x)$, are the same as the basis functions, $u_x^i(x_s)$ or $u_z^j(x_s)$, are given by

$$w_x^i(x) = \begin{cases} \cos\left(\dfrac{(2n-1)\pi x}{a_i}\right) & (n=1,2,\cdots,M_i) \\ & x \in \Gamma_3 \\ \sin\left(\dfrac{n\pi(x-w_i/2)}{s}\right) & (n=1,2,\cdots,M_i) \\ & x \in \Gamma_1, \Gamma_2 \end{cases} \quad \text{(A5)}$$

$$w_z^i(x) = \begin{cases} \sin\left(\dfrac{(2n-1)\pi x}{a_i}\right) & (n=1,2,\cdots,M_i) \\ & x \in \Gamma_3 \\ \cos\left(\dfrac{n\pi(x-w_i/2)}{s}\right) & (n=0,1,\cdots,M_i) \\ & x \in \Gamma_1, \Gamma_2 \end{cases} \quad \text{(A6)}$$

VI. ACKNOWLEDGMENT

The authors thank Prof. K. Atsuki and Dr. N. Kishi of the University of Electro-Communications for their helpful discussions.

REFERENCES

[1] E. Yamashita, B. W. Wang, K. Atsuki and K. R. Li, "Effects of side-wall grooves on transmission characteristics of suspended striplines," *IEEE Trans. Microwave Theory Tech.*, vol. MTT-33, no. 12, pp. 1323–1328, Dec. 1985.

[2] C. H. Chan, K. T. Ng and A. B. Kouki, "A mixed spectral-domain approach for dispersion analysis of suspended planar transmission lines with pedestals," *IEEE Trans. Microwave Theory Tech.*, vol. 37, no. 11, pp. 1716–1723, Nov. 1989.

[3] F. Alessandri, U. Goebel, F. Melai and R. Sorrentino, "Theoretical and experimental characterization of nonsymmetrically shielded coplanar waveguides for millimeter-wave circuits," *IEEE Trans. Microwave Theory Tech.*, vol. 37, no. 12, pp. 2020–2027, Dec. 1989.

[4] E. Yamashita and K. Atsuki, "Strip line with rectangular outer conductor and three dielectric layers," *IEEE Trans. Microwave Theory Tech.*, vol. MTT-18, no. 5, pp. 238–244, May 1970.

[5] T. K. Lee, H. Ling and T. Itoh, "Boundary element characterization of coplanar waveguides," *IEEE Microwave Guided Wave Lett.*, vol. 1, no. 12, pp. 385–387, Dec. 1991.

[6] K. A. Michalski and D. Zheng, "Rigorous analysis of open microstrip lines of arbitrary cross section in bound and leaky regime," *IEEE Trans. Microwave Theory Tech.*, vol. 37, no. 12, pp. 2005–2010, Dec. 1989.

[7] B. Toland and T. Itoh, "Boundary element analysis of a trapezoidal transmission line," *IEEE Microwave and Guided Wave Lett.*, vol. 1, no. 12, pp. 391–392, Dec. 1991.

[8] T. N. Chang and C. H. Tan, "Analysis of a shielded microstrip line with finite metallization thickness by the boundary element method," *IEEE Trans. Microwave Theory Tech.*, vol. 38, no. 8, pp. 1130–1132, Aug. 1990.

[9] L. Zhu and E. Yamashita, "New method for the analysis of dispersion characteristics of various planar transmission lines with finite metallization thickness," *IEEE Microwave Guided Wave Lett.*, vol. 1, no. 7, pp. 164–166, July 1991.

[10] L. Zhu and E. Yamashita, "Accurate analysis of various planar transmission lines with finite metallization thickness using eigen-function weighted boundary integral equation method," *IEICE Trans. Electron.*, vol. E75-C, no. 2, pp. 259–266, Feb. 1992.

[11] R. F. Harrington, *Time-Harmonic Electromagnetic Fields*. New York: McGraw-Hill, 1961.

[12] J. Bornemann, "A scattering-type transverse resonance technique for the calculation of (M) MIC transmission line characteristics," *IEEE Trans. Microwave Theory Tech.*, vol. 39, no. 12, pp. 2083–2088, Dec. 1991.

[13] R. R. Mansour and R. Macphie, "A unified hybrid-mode analysis for planar lines with multilayer isotropic/anisotropic substrates," *IEEE Trans. Microwave Theory Tech.*, vol. MTT-35, no. 12, pp. 1382–1391, Dec. 1987.

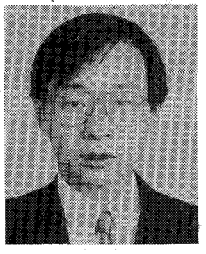

Lei Zhu (S'92) was born in Jiangsu, China, on June 19, 1963. He received the B.E. and the M.E. degrees from the Nanjing Institute of technology, Nanjing, China in 1985 and 1988, respectively. He is presently working towards the Ph.D. degree at the University of Electro-Communications, Tokyo, Japan.

Mr. Zhu's research interests include analytical and numerical methods for the solution of boundary value problems of electromagnetics, and design of various components and leaky-wave antennas.

Eikichi Yamashita (M'66–SM'79–F'84) was born in Tokyo, Japan, on February 4, 1933. He received the B.S. degree from the University of Electro-communications, Tokyo, Japan, and the M.S. and Ph.D. degrees from the University of Illinois, Urbana, all in electrical engineering, in 1956, 1963, and 1966, respectively.

From 1956 to 1964, he was a member of the research staff on millimeter-wave engineering at the Electrotechnical Laboratory, Tokyo, Japan. While on leave from 1961 to 1963 and from 1964 to 1966, he studied solid-state devices in the millimeter-wave region at the Electro-Physics Laboratory, University of Illinois. He became Associate Professor in 1967 and Professor in 1977 in the Department of Electronic Engineering, the University Electro-communications, Tokyo, Japan. His research work since 1956 has been principally on applications of electromagnetic waves such as various microstrip transmission lines, wave propagation in gaseous plasma, pyroelectric-effect detectors in the submillimeter-wave region, tunnel-diode oscillators, wide-band laser modulators, various types of optical fibers, ad ultra-short electrical pulse propagation on transmission lines.

Dr. Yamashita was Chairperson of the Technical Group on Microwaves, IE-ICE, Japan, for the period 1985–1986 and Vice-Chairperson, Steering Committee, Electronics Group, IEICE, for the period 1989–1990. He has served as Associate Editor of the IEEE TRANSACTIONS ON MICROWAVE THEORY AND TECHNIQUES during the period 1980–1984. He was elected Chairperson of the MTT-S Tokyo Chapter for the period 1985–1986 and served as Chairperson of the International Steering Committee, 1990 Asia-Pacific Microwave Conference, held in Tokyo. He also edited the book, *Analysis Methods for Electromagnetic Wave Problems*, published by Artech House, Co..